scientific reports

OPEN

Microwave-assisted preparation of polysubstituted imidazoles using Zingiber extract synthesized green Cr_2O_3 nanoparticles

Leila Kafi-Ahmadi[1], Shahin Khademinia[2], Ahmad Poursattar Marjani[3]✉ & Ehsan Nozad[3]

Cr_2O_3 nanoparticles were prepared using Zingiber officinal extract which were used as an efficient and reusable catalyst in the practical synthesis of polysubstituted imidazoles by means of a convenient reaction of aromatic aldehydes with ammonium acetate and benzil under microwave irradiation and H_2O as solvent. The structure of the compounds was studied by IR and ^{1}H-NMR spectrum. The most important benefits of this process are operational simplicity, reasonable reaction times, and excellent yield of products. The results show that the optimal conditions for the formation of imidazole derivatives are as follow: power of 400 W, reaction time of 4–9 min, H_2O as a solvent, and 15 mmol of catalyst amount.

In recent years, metal and metal oxide nanomaterials have attracted significant attention in various synthesis processes[1]. Functional nanomaterials have stupendous applications in different areas such as biomedical, environment, food preservation, and health care, cosmetics, water purification, fuel cells, drug delivery and gene delivery, defense, chemical industries, space industries, ceramics, energy, sensors, single-electron transistors, textiles, agriculture, solar cells, catalysis, light emitters, fuel, and antimicrobial[2]. Among the metal oxides, Cr_2O_3 is more considerable due to their specific thermodynamic stability, antiferromagnetic, chemical resistance, hardness, and good catalytic reusability attributes[3].

Chromium oxide has various crystal states such as CrO_2 (rutile), CrO_3, CrO_4, Cr_2O_3 (corundum), Cr_2O_5, and Cr_5O_{12}. In this respect, Cr_2O_3 is known to be the most stable magnetic-dielectric oxide[4]. Cr_2O_3 depicts p-type and n-type semiconductor behavior[5] that all these characteristics make Cr_2O_3 a suitable material for a variety of industrial applications.

Based on previous reports, numerous studies have been accomplished about applications of Cr_2O_3 nanoparticles (NPs) involving sensors[6], catalysis[7], protective coating and green pigment[8], fuel cell[9], solar cell[10], piezoelectric devices[11], photocatalysis[12]. Moreover, Cr_2O_3 NPs are known to be one of the significant compounds in the field of medicine and pharmacy, having anticancer, antibacterial, antileishmanial, and antioxidant specifications[5].

Various techniques are used to synthesize Cr_2O_3 nanoparticles such as hydrothermal[13], solid thermal decomposition[14], combustion[15], sol-gel[16], precipitation-gelation[17], oxidation of chromium in oxygen[18], sonochemical[19] mechanochemical reaction and subsequent heat treatment[20], laser induced deposition[21], and biological methods[22]. Besides, there are several reports introducing the synthesis of nanoparticles by green method using extracts, including CuO[23], Cu[24], AgCl[25], Ag[26], etc.

In contrast to chemical and physical methods, biological approaches are critical because of their rapid, ease in use, economic production and less generation of waste products. Different and nearly all parts of a plant such as flowers, fruit, and leaves are consisted of bio-based components like flavonoids, alkaloids, etc. The mentioned components prove the rich ingredients of the plants and exhibit their great potential to be used as a base for medical and pharmaceutical applications[27].

A research has been accomplished on the extract of Callistemon Viminalis and examining its possible usage as a capping reagent for Cr_2O_3 NPs synthesis[22]. The fabrication of Cr_2O_3 NPs was investigated in another research through *Callostemon viminalis* extraction that were used for biological purposes[5]. In another study by Sharma and their group[28], the extract obtained from the Cannabis Sativa leaves was used for Cr_2O_3 NPs preparation.

[1]Department of Inorganic Chemistry, Faculty of Chemistry, Urmia University, Urmia, Iran. [2]Department of Inorganic Chemistry, Faculty of Chemistry, Semnan University, Semnan, Iran. [3]Department of Organic Chemistry, Faculty of Chemistry, Urmia University, Urmia, Iran. ✉email: a.poursattar@urmia.ac.ir; a.poursattar@gmail.com

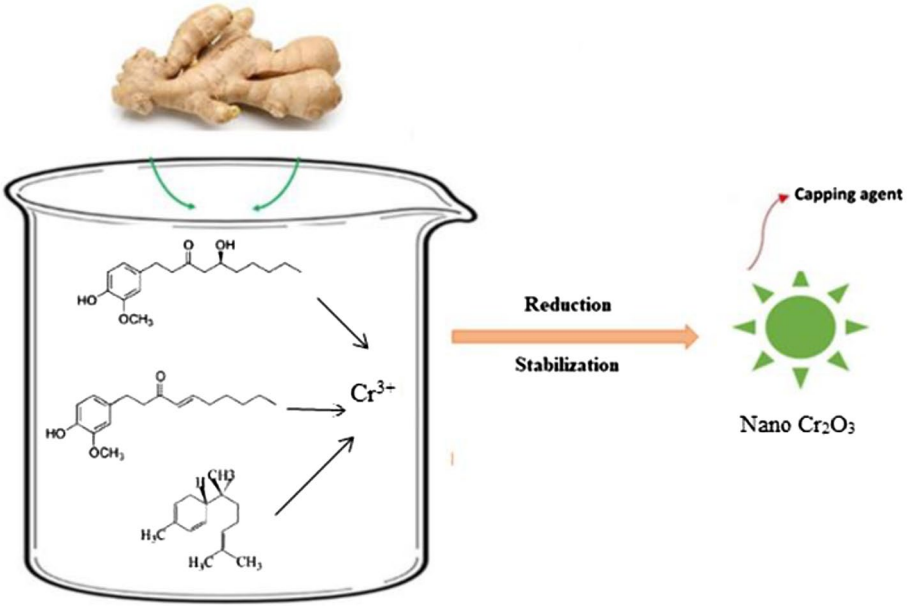

Figure 1. Schematic representation of the biosynthetic pathway of Cr_2O_3 nanoparticles using *Zingiber officinale* extract.

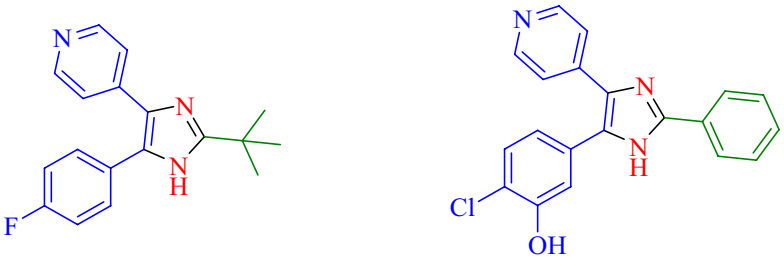

Figure 2. Some biological heterocyclic compounds containing imidazole moieties.

Sphere-shaped Cr_2O_3 NPs were fabricated with Hyphaene thebaica extraction in other research[29]. The investigations in this field are vast, and in this respect, the extractions of Artemisia herba-alba leaves[30], Melia Azedarach fruits[30], and Nephelium Lappaceum[31] were used for Cr_2O_3 synthesizing. It has been reported that the leaves of Opuntia Ficus can be a potential reducing, and capping agent for Cr_2O_3 preparation[32]. Rhamnus Virgata[33], Ipomoea batatas[34] and Tridax Procumbens[35] are among the other reported plants that their extraction has been used for Cr_2O_3 NPs production.

Effect of pH, temperature, concentration of extract and reaction time on the green synthesis of nanoparticles have been investigated. For instant, changing the pH value of the reaction mixture solution changes the grain size of the synthesized sample. Synthesis of nanoparticles in the green rout requires less than 100 °C. The temperature range governs the formed nanoparticles nature[36]. Plant extract is a complex concoction of several phytochemicals, for example, phenolics, sugars, flavonoids, xanthones, and several others. In general, it is said that hydroxyl-rich phenolics act as reducing agents for metal ions, but little is discussed about the stabilizing ligands of metal nanoparticles (NPs). Thus, despite the popularity of plant extract-mediated synthesis of NPs, the phytochemical basis of the process and the exact mechanism are still unclear[37].

Zingiber, known as Ginger as well is one of the mainly used herbals containing bioactive compounds such as phenols, paradols, curcumin, etc. Ginger is associated with the Zingiberaceae family involving about 800 species.

The ginger is used for therapeutic purposes in as much as its phytochemical's components. This characteristic of ginger is very effective on bacterial pathogens in a wide range[38]. Zingiber extract can perform both as a reducing and stabilizing agent (Fig. 1).

The *N*-heterocyclic compounds are considered as a group of precious compounds existing in many structures exhibiting potential features in medical materials[39,40]. In the group of numerous heterocyclic structured materials, imidazoles are very substantial within biological compounds[41]. The imidazole structural scaffolds and analogs are used as antibacterial, herbicides, fungicides, anti-inflammatory, antitumor, therapeutic, and plant growth regulators agents[42]. Moreover, this class of compound act as an inhibitor of B-Raf, p38 MAP kinase, and glucagon receptors[43] (Fig. 2).

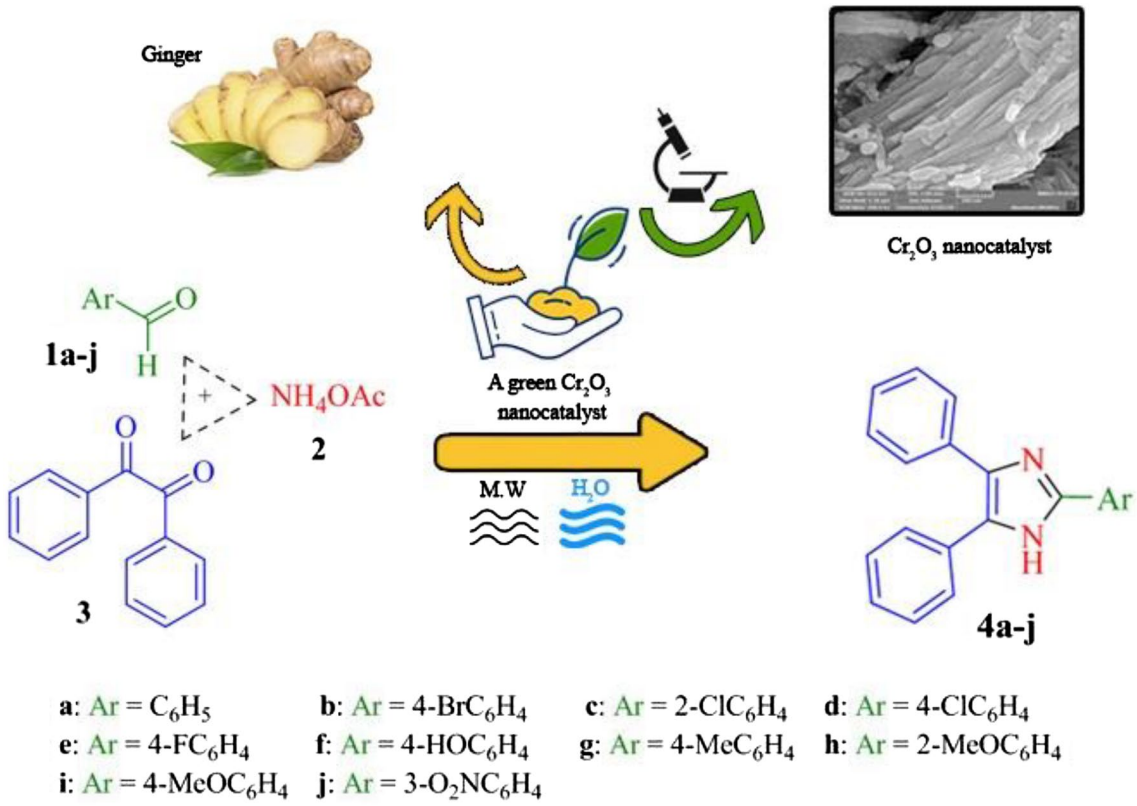

Figure 3. Synthesis of imidazole derivatives **4a–j** with Cr_2O_3 as catalyst under microwave irradiation.

Such compounds are used as the base of some other structures. In this respect, imidazole synthesis obtains a high effect in the preparation of medically essential compounds. Several improved methods and procedures for the preparation of polysubstituted imidazoles have been reported, that best-reported route is a three-component, cyclo-condensation reaction between aldehyde, benzil, and NH_4OAc in the presence of a different catalyst such as zeolite HY/silica gel[44], ionic liquid[45,46], iodine[47], sodium bisulfite[48], $ZrCl_4$[49], $Yb(OTf)_3$[50]. Alternative methods with the application of microwave source energy and appropriate catalyst through using 1,2-diketone and aldehyde for imidazole synthesis have been proposed such as MW/Silica-gel[51], glyoxylic acid[52], $InCl_3.3H_2O$[53].

Using the microwave energy source within the synthesis of different compounds is an environmental friendly technique. The energy of microwaves is high; therefore, short times are needed for the accomplishment of the reactions, hence, having great superiority from the time point of view. In this respect, microwave technology has an ascending usage in synthesizing various compounds[54].

In continuation of our investigation towards designing novel catalysts in the synthesis of heterocyclic compounds[55–60], we synthesized Cr_2O_3 nanoparticles using Zingiber officinal extract, and used it as a Lewis acid catalyst for the preparation of polysubstituted imidazoles (Fig. 3). To the best of the authors' knowledge, this study is the first investigation in this manner. Besides, the significance of the present study is the green and facile synthesis of the Cr_2O_3 nanomaterial, and application of the synthesized compound as efficient catalyst for the preparation of imidazole derivatives **4a–j**.

Experimental

Materials and instruments. The chemicals were obtained from Merck company, and no excess purification was carried out. Zingiber was purchased from local market, Urmia, West Azerbaijan, Iran and the collection of plants materials used in current study complied with institutional, national or international guidelines. X-ray Powder Diffraction (XRPD) pattern was recorded by the X-ray diffractometer (D5000 Siemens AG, Germany) using CuKα radiation to make phase identification. The FESEM image was taken on a Hitachi model S-4160 for morphology study. FT-IR spectra were obtained with FT-IR spectrometer (Bruker, Germany). Thin-layer chromatography using petroleum ether/ethyl acetate (9:1) mixture was used to evaluate the purity of the products. ^{1}H-NMR spectra of compounds were run on a Bruker Avance DRX-400 spectrometer using tetramethylsilane as an internal standard and dimethyl sulfoxide-d_6 as solvent. Microwave-assisted procedures were performed in the Milestone Microwave Oven.

Preparation of plant extract. The purchased dried root of Zingiber was ground and a fine powder was obtained. Then, 300 mg of the prepared powder was poured into 30 mL of distilled water. The mixture was stirred at 70 °C for 20 min. Finally, the extraction was cooled to room temperature and filtered out. The product was kept at decreased temperature (4 °C) for subsequent use (Fig. 4).

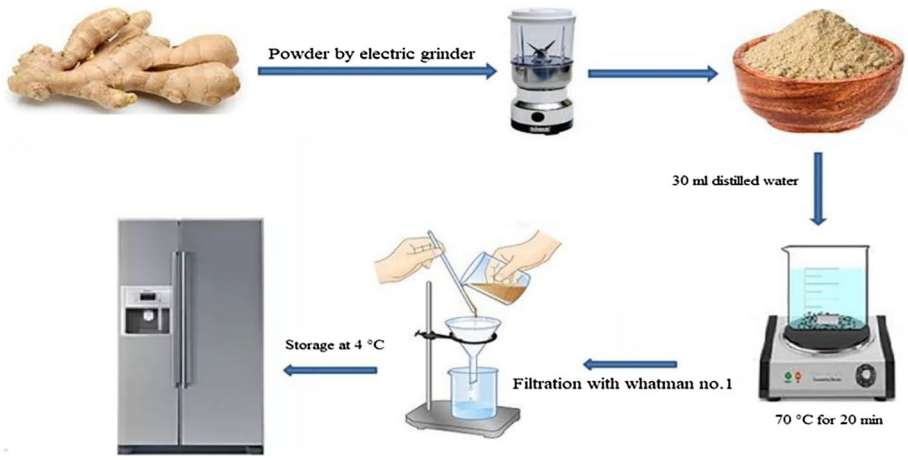

Figure 4. The synthesis scheme of extraction of ginger.

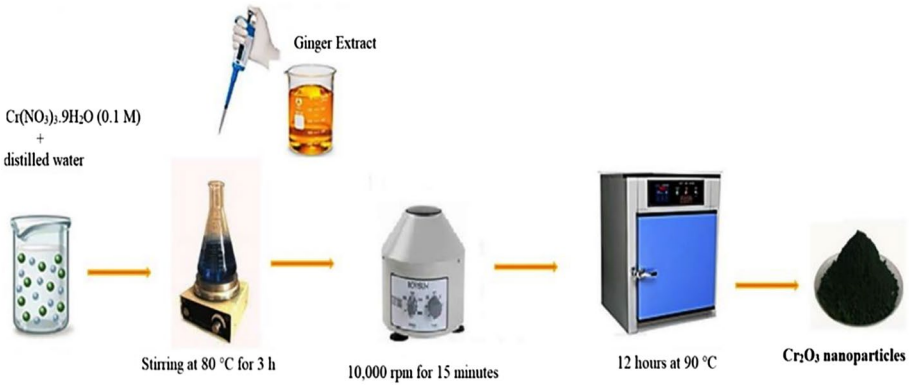

Figure 5. The stepwise synthesis pathway of Cr_2O_3 nanoparticles.

Green synthesis of Cr_2O_3 nanoparticles. Ginger aqueous extract (3 mL) was added to $Cr(NO_3)_3{\cdot}9H_2O$ (0.1 M) under continuous stirring. Sodium hydroxide 2 M solution was used to adjust the pH on 12 at 80 °C. The formed precipitate was centrifuged for 15 min, then rinsed with distilled water, and dried at 90 °C for 12 h in an oven (Fig. 5).

General procedure for the synthesis of imidazole derivatives 4a–j. A mixture of aromatic aldehydes (**1a–j**, 1 mmol), ammonium acetate (**2**, 3 mmol), and benzil (**3**, 1 mmol) in water (2 mL), and Cr_2O_3 nanoparticles (15 mmol) were prepared. The obtained mixture was kept under agitation and microwave (400 W) was used to treat the mixture with irradiation for an appropriate time (Table 5, reaction time in the range of 4–9 min). TLC was used to investigate the reaction progress (ethyl acetate/petroleum ether; 1:9 as eluent). Next, the obtained mixture temperature was decreased to room temperature by adding it to an ice containing beaker. Afterward, the achieved product was filtered out under reduced pressure, following by rinsing with water for several times and drying. Finally, recrystallization was done using ethanol in order to obtain a highly pure products **4a–j** (89–98% yield).

Results and discussions

Powder X-ray diffractometry analysis. XRD pattern of the prepared catalyst is shown in Fig. 6, and nine different Bragg's diffraction peaks can be observed associated with crystal planes of (012), (104), (110), (113), (024), (116), (214), (220), and (306) at $2\theta = 24.3°$, 33.7°, 36.3°, 41.4°, 50.1°, 54.8°, 63.5°, 76.7°, and 79.0° respectively. The obtained pattern for Cr_2O_3 nanoparticles is in agreement with Joint Committee on Powder Diffraction Standards (JCPDS) 38–1479[61]. No peak related to any impurity was seen that confirm the high purity of the particles.

In addition, the mean crystallite size of the Cr_2O_3 sample was evaluated using the Scherrer formula as follows:

$$D = K\lambda/(\beta \cos\theta)$$

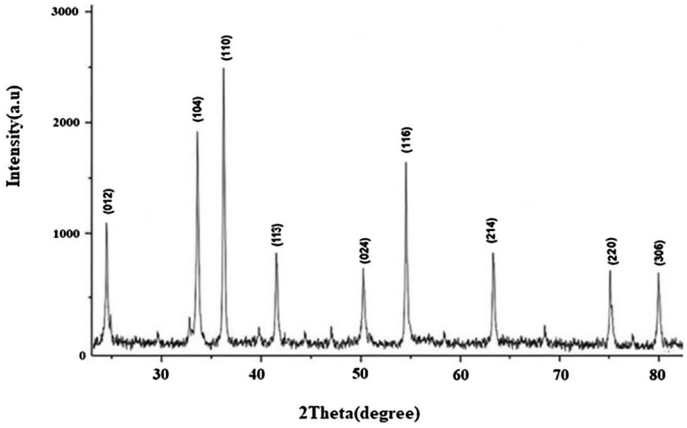

Figure 6. XRD analysis of green synthesized Cr_2O_3 nanoparticles.

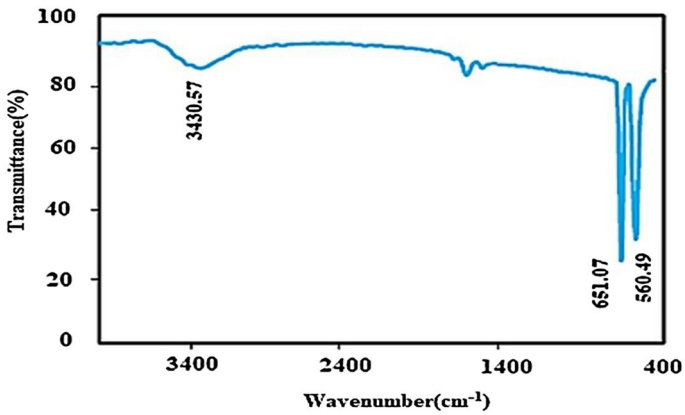

Figure 7. FT-IR spectrum of the green synthesized Cr_2O_3.

where K (0.9), λ (1.54056 Å), β, and θ are Scherer constant, X-ray radiation wavelength, full peak width at half maximum, and Bragg diffraction angle, respectively. In this respect, Cr_2O_3 crystallite size, in average was calculated at about 14 nm.

FT-IR analysis. The FT-IR spectrum of Cr_2O_3 nanoparticles is illustrated in Fig. 7. The peaks below 1000 cm^{-1} may be due to the inter-atomic vibrations and in this study, may be associated with the Cr–O bands. This phenomenon can be seen in the spectrum of the metal oxide frequently. The high intensity of the peaks of Cr_2O_3 bands indicates the good crystalline nature of the material. Two sharp peaks at 651 cm^{-1} and 560 cm^{-1} could be related to Cr–O stretching modes are clear evidence of the attendance of the crystalline Cr_2O_3[62]. The broadband around 3400 cm^{-1} can be due to the hydroxyl groups of water.

Morphology analysis. Figure 8, shows the FESEM image of the as-synthesized nanomaterial. It can be seen that the main morphology of the material is a mixture of rod and particle. TEM image exhibits that the diameter size of the as-prepared sample is 30–40 nm.

Magnetic property. Figure 9, shows the hysteresis loop for a sample at room temperature. Accordingly, the synthesized particle possesses a soft magnetic nature. The value of magnetization saturation (M_s) is about 42 emu/g. Remnant magnetization M_r is the magnetization strength of the materials remaining after removing the external magnetic field or descending to a zero level. M_{rs} as the square of magnitudes is achieved using ($M_{rs} = M_r/M_s$) formula. Magnetic parameters are summarized in Table 1. The particle with homogenous distribution and magnetization with no inter-grain interactions will give a M_{rs} below 0.5. This value can be interpreted through multiple domains of the structure formed due to the exchange coupling among adjoining grains. In this study, the M_{rs} is 0.19 affirming that the sample has no preferred direction in magnetization. Moreover, a normal (S-shaped) narrow hysteresis loop was observed as well. The narrow loop is an indication of a low coercivity. Therefore, the prepared sample can be easily demagnetized.

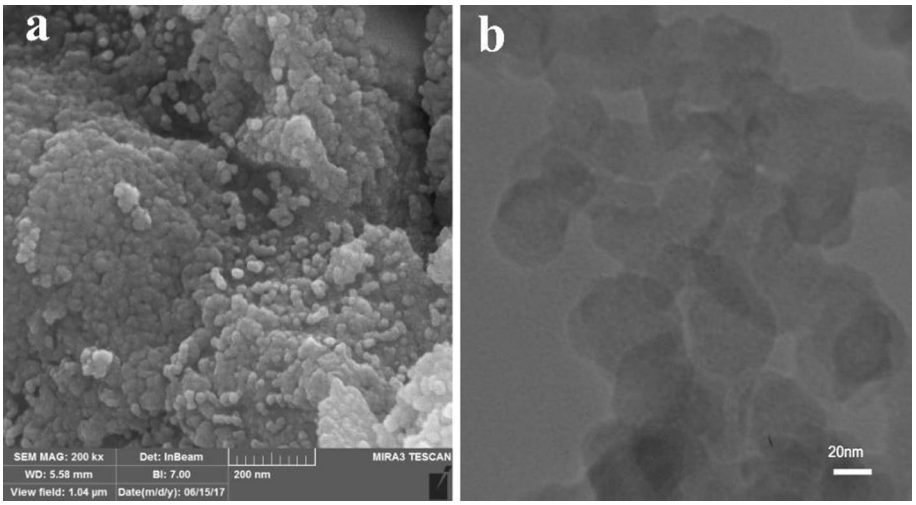

Figure 8. FESEM (**a**) and TEM (**b**) image of synthesized Cr_2O_3.

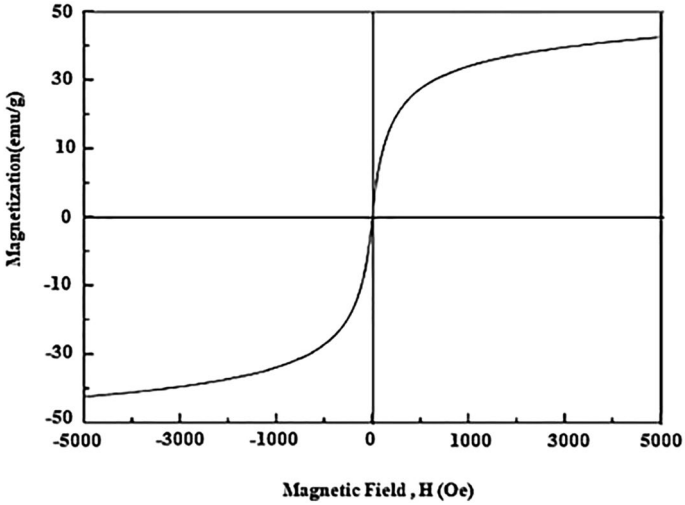

Figure 9. VSM curves of the as-synthesized nanomaterial.

Sample	M_r (emu/g)	M_s (emu/g)	$M_{rs} = M_r/M_s$	H_c (Oe)
Cr_2O_3	4.9	42.3	0.115	50.7

Table 1. Magnetic parameters of the sample.

Evaluation of the catalytic activity of the as-prepared Cr_2O_3 nanoparticles for the synthesis of imidazoles 4a–j

The synthesized catalyst was evaluated, and their efficiency in the imidazoles preparation was studied. The one-pot, three-component reaction of benzaldehyde (**1a**), ammonia source (**2**, $AcONH_4$), and benzil (**3**), was chosen as a trial reaction. Some prerequisite conditions were assessed by initial experiments regarding the optimum conditions.

Different aryl aldehydes **1a–j** were used to evaluate the reaction process. Manifestly, in the reactions with no nanocatalyst usage, no considerable progress was observed. Hence, in order to investigate the as-prepared nanocatalyst effect in the present procedure, different amounts of catalyst ranging from 5 to 25 mmol was applied (Table 2). Interestingly, excellent yield was observed using 15 mmol of nanocatalyst (Table 2, entry 4) in water as a green solvent.

Entry	Catalyst (mmol)	Time (min)	Yield (%)
1	–	6	–
2	5	6	35
3	10	6	51
4	**15**	**6**	**97**
5	20	6	97
6	25	6	97

Table 2. Effect of Cr_2O_3 nanoparticles as nanocatalyst on the synthesis yields of compound **4a**. Reaction conditions: Benzaldehyde (**1a**, 1 mmol), $AcONH_4$ (**2**, 3 mmol), benzil (**3**, 1 mmol), and catalyst in H_2O (2 mL) under microwave irradiation (400 W). Significant values are in bold.

Entry	Catalyst (mmol)	Microwave power (W)	Time (min)	Yield[a] (%)
1	15	200	6	65
2	15	300	6	80
3	**15**	**400**	**6**	**97**
4	15	500	6	97

Table 3. Effect of microwave power on the synthesis of trial reaction. Reaction conditions: **1a** (1 mmol), **2** (3 mmol), **3** (1 mmol), and catalyst (15 mmol) in water (2 mL). Significant values are in bold. [a]Isolated yield.

Entry	Solvent	Yield (%)
1	–	–
2	Et_2O	–
3	$CHCl_3$	–
4	DMSO	14
5	THF	17
6	DMF	33
7	CH_3CN	28
8	**H_2O**	**97**
9	EtOH	89
10	H_2O/EtOH (1:1)	90
11	H_2O/EtOH (2:1)	91

Table 4. Optimization of reaction conditions for the synthesis of compound **4a**. The reaction of **1a** (1 mmol), **2** (3 mmol), **3** (1 mmol), catalyst (15 mmol) and solvent (2 mL) under microwave irradiation was carried out. Significant values are in bold.

Moreover, increase in the amount of catalyst had no significant effect on the outcome (Table 2, entries 5 and 6). Also, the lower quantities of the nanocatalyst afford moderate yield of the product at a longer reaction time (Table 2, entries 2 and 3).

Microwave effect with power in the range of 200–500 W was exanimated (Table 3). According to the results, 400 W was chosen as the optimized power for synthesizing substituted imidazole derivatives.

In addition, the solvent effect was assessed, and the results are shown in Table 4. No progress in the reaction was observed without a solvent, even after a considerable time. This finding affirms the requirement for an appropriate solvent.

According to the results, no considerable reaction progress was observed while using nonpolar solvents such as Et_2O. However, by using polar aprotic solvents such as DMF, low yields were achieved. Nonetheless, polar protic solvents like water, and ethanol had a better effect and the yields of 97% and 89% were obtained for H_2O and EtOH respectively.

Encouraged by this success, using the obtained optimum reaction parameters, the scope and efficiency of this approach were demonstrated for the synthesis of polysubstituted imidazoles **4a–j** and the results are outlined in Table 5. As can be seen, the extension of substrate scope, the different aryl aldehyde containing the various functional groups on the benzene ring such as halogens, hydroxyl, methyl, methoxy, and nitro was examined with ammonium acetate and benzil under the optimized conditions for imidazoles synthesis. However, aryl aldehyde with electron-withdrawing groups, like nitro, require more reaction time to form the product **4j** (89%).

Entry	Aromatic aldehyde	Product	Time (min)	Yield[a] (%)	M.p.[b] (°C)	
					Found	Refs.
1	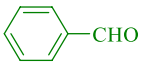	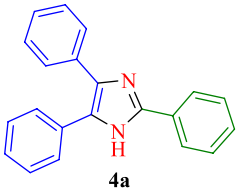 **4a**	6	97	269–271	270–272[63]
2	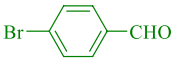	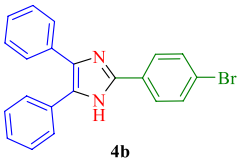 **4b**	5	94	249–251	250–252[64]
3	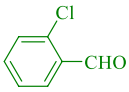	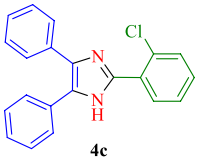 **4c**	6	92	197–199	198–200[65]
4	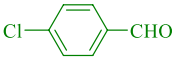	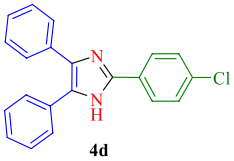 **4d**	5	93	260–263	260–265[63]
5	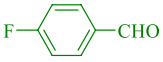	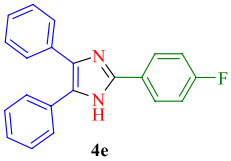 **4e**	6	94	238–240	239–241[66]
6	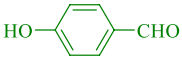	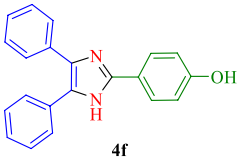 **4f**	4	97	234–236	235–237[63]
7	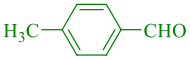	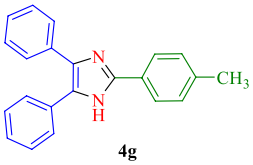 **4g**	4	96	230–233	232–234[64]
8	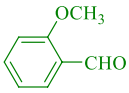	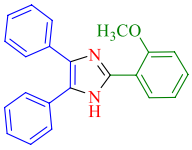 **4h**	5	96	207–209	208–210[65]
9	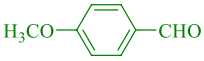	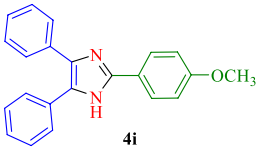 **4i**	4	98	219–221	220–223[67]

Continued

Entry	Aromatic aldehyde	Product	Time (min)	Yield[a] (%)	M.p.[b] (°C)	
					Found	Refs.
10	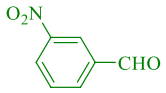	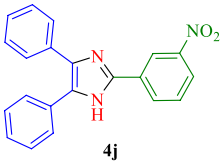 **4j**	9	89	300–303	302–304[65]

Table 5. Cr_2O_3 catalyzed the synthesis of imidazole derivatives **4a–j**. [a]Isolated yields. [b]The measured melting points comparison with those in literature confirmed the products.

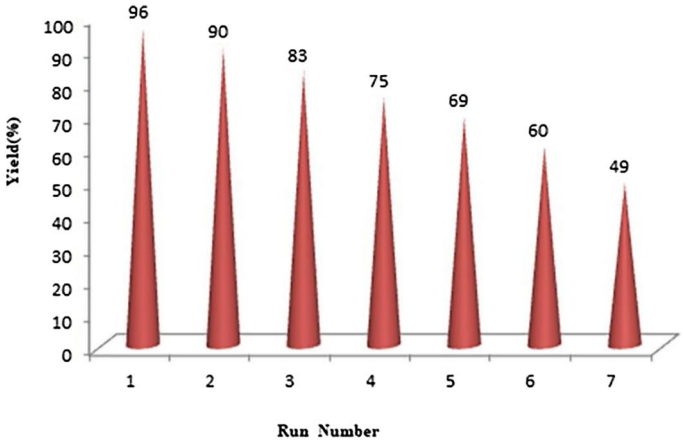

Figure 10. Reusability of Cr_2O_3 in the synthesis of compound **4a**.

Entry	Catalyst	Time (min)	Yield (%)
1	Schiff base nickel complex (Ni–C)	20	90[68]
2	ZrO_2–Al_2O_3	20	99[69]
3	Rochelle salt	10	93[70]
4	Fe_3O_4	20	85[71]
5	$TiCl_4$–SiO_2	10	93[72]
6	$CuCl_2{\cdot}2H_2O$	13	87[54]
7	Triflate	30	96[73]
8	BTPPC	10	92[74]
9	$MgAl_2O_4$	14	93[75]
10	Cr_2O_3	6	97 (this work)

Table 6. Comparison of various heterogeneous catalysts in the formation of compound **4a**.

Recycling of Cr_2O_3 nanoparticles as a catalyst under microwave irradiation

The catalytic performance of Cr_2O_3 after multiple cycles of usage was investigated. It has been proved that the prepared nanocatalyst can be used even after 6 runs with no considerable decrease in its efficiency (Fig. 10).

To show the advantages of the current work, we compared the results with literature. As shown in Table 6, Cr_2O_3 is the most efficient catalyst and gives excellent product yields in reduced reaction times. In addition, the merit of Cr_2O_3 is its recyclability and easy work-up.

Figure 11, presents a suggested synthesis mechanism for the imidazoles. In the first step, the catalyst increased the electrophilicity of the aromatic aldehydes carbonyl groups **1a–j**. Then, the ammonia's nitrogen (**2**, obtained from ammonium acetate) intermolecular nucleophilic attack to the activated center of the carbonyl group generated diamine intermediate **I**. Next, intermediate **II** is produced by nucleophilic attack of the intermediate **I** nitrogen to the carbonyl groups of benzil (**3**). Afterwards, the typical intramolecular condensation of the intermediate **II** followed by a heterocyclization, afforded the intermediate **III**, while the removal of two water molecules occurs and the conjugate intermediate **IV** is obtained. Finally, the aromatization of intermediate **IV**

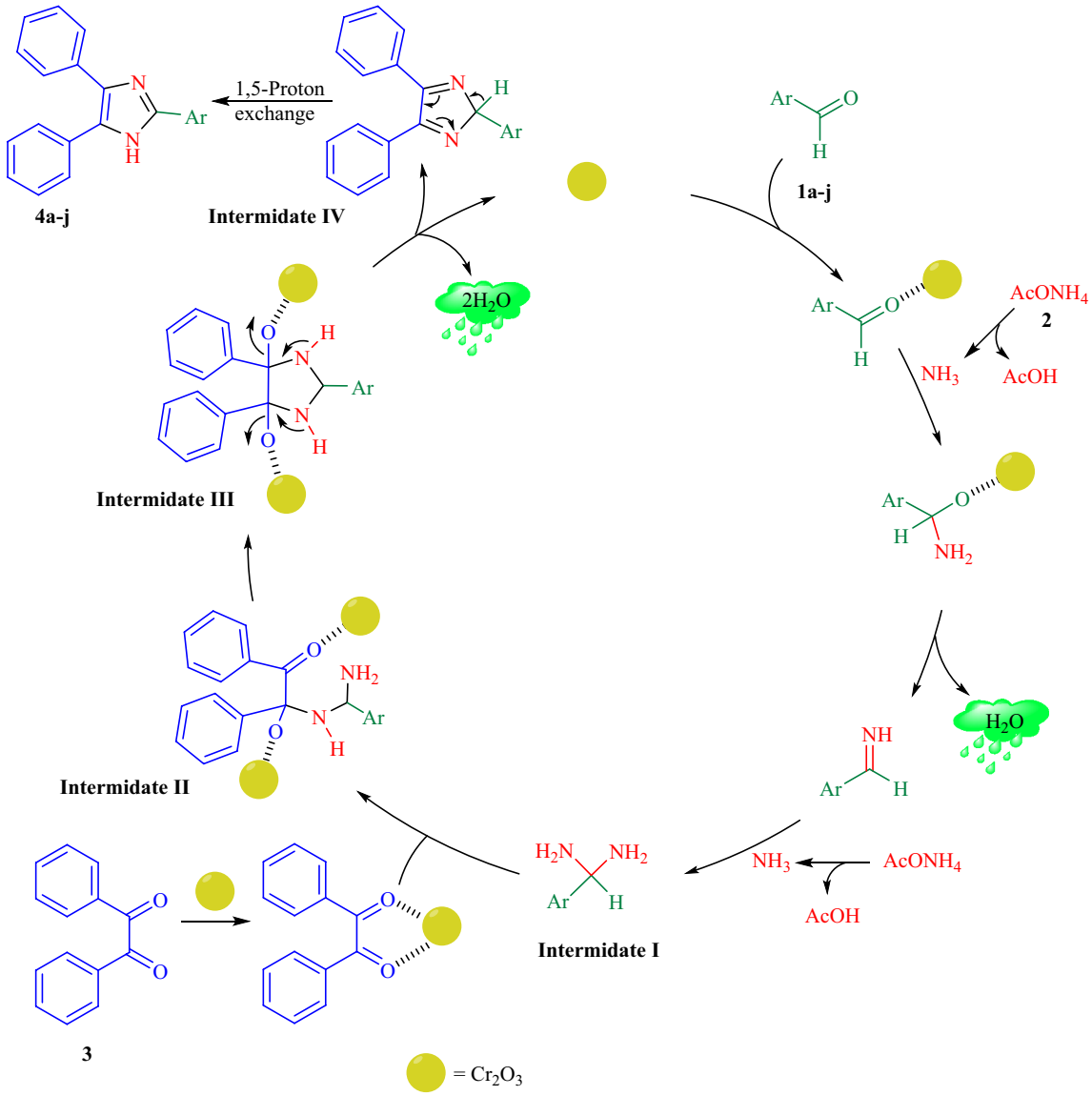

Figure 11. Plausible reaction mechanism for the synthesis of imidazole derivatives.

takes place leads to the corresponding five membered heterocyclic compounds as the desired imidazoles **4a–j** under 1,5-proton exchange.

Conclusion

In summary, an easy, cost-effective, and eco-friendly biological successful technique was used for synthesizing of Cr_2O_3 nanostructures using $Cr(NO_3)_3.9H_2O$ as a precursor, and Zingiber officinal extract as a stabilizing and reducing agent. The green synthesized Cr_2O_3 nanoparticles was characterized using SEM, XRD, TEM, FT-IR, and VSM analyses. The mean crystallite size was 14 nm, as confirmed by the analysis of XRD pattern using the Scherrer equation. Then, the synthesized Cr_2O_3 was used as a heterogeneous Lewis acid catalyst for efficient synthesis of imidazole derivatives by condensation of aromatic aldehydes took place with ammonium acetate and benzil in the attendance of a catalytic amount of Cr_2O_3, and H_2O as solvent under microwave illumination. High reaction yield (97%) was obtained when benzaldehyde was used as aldehyde derivative. The prepared nanocatalyst was recovered and its high efficiency even after six runs was proved. Reasonable reaction times, excellent yields, easy work-up, and the absence of any hazardous and volatile organic solvents were the main merits of this benign protocol.

Data availability

All data generated or analyzed during this study are included in this published article [and its supplementary information files].

Received: 9 August 2022; Accepted: 14 November 2022
Published online: 19 November 2022

References

1. Khan, I., Saeed, K. & Khan, I. Nanoparticles: Properties, applications and toxicities. *Arab. J. Chem.* **12**, 908–931 (2019).
2. Ghotekar, S., Pagar, K., Pansambal, S., Murthy, H. C. A. & Oza, R. A review on eco-friendly synthesis of $BiVO_4$ nanoparticle and its eclectic applications. *Adv. J. Sci. Eng.* **1**, 106–112 (2020).
3. Ghotekar, S., Pansambal, S., Bilal, M., Pingale, S. S. & Oza, R. Environmentally friendly synthesis of Cr_2O_3 nanoparticles: Characterization, applications and future perspective—A review. *Case Stud. Chem. Environ. Eng. (CSCEE)* **3**, 100089 (2021).
4. Abdullah, M. M., Rajab, F. M. & Al-Abbas, S. M. Structural and optical characterization of Cr_2O_3 nanostructures: Evaluation of its dielectric properties. *AIP Adv.* **4**, 027121 (2014).
5. Hassan, D. *et al.* Physiochemical properties and novel biological applications of *Callistemon viminalis*-mediated α-Cr_2O_3 nanoparticles. *Appl. Organomet. Chem.* **33**, e5041 (2019).
6. Ding, C. *et al.* Ordered large-pore mesoporous Cr_2O_3 with ultrathin framework for formaldehyde sensing. *ACS Appl. Mater. Interfaces* **9**, 18170–18177 (2017).
7. Wang, S., Murata, K., Hayakawa, T., Hamakawa, S. & Suzuki, F. Dehydrogenation of ethane with carbon dioxide over supported chromium oxide catalysts. *Appl. Catal. Gen.* **196**, 1–8 (2000).
8. Ku, R. C. & Winterbottom, W. L. Electrical conductivity in sputter-deposited chromium oxide coatings. *Thin Solid Films* **127**, 241–256 (1985).
9. Linder, M. *et al.* Cr_2O_3 scale growth rates on metallic interconnectors derived from 40,000 h solid oxide fuel cell stack operation. *J. Power Sour.* **243**, 508–518 (2013).
10. Sim, J. K. *et al.* Efficiency enhancement of CIGS compound solar cell fabricated using homomorphic thin Cr_2O_3 diffusion barrier formed on stainless steel substrate. *Appl. Surf. Sci.* **389**, 645–650 (2016).
11. Jianhua, L. I. & Qingchi, S. U. N. Effects of Cr_2O_3 doping on the electrical properties and the temperature stabilities of PZT binary piezoelectric ceramics. *Rare Met.* **27**, 362–366 (2008).
12. Su, J., Xue, H., Gu, M., Xia, H. & Pan, F. Synthesis of spherical Cr_2O_3 nanoparticles by a microwave refluxing method and their photocatalytic properties. *Ceram. Int.* **40**, 15051–15055 (2014).
13. Moezzi, A., McDonagh, A. M. & Cortie, M. B. Zinc oxide particles: Synthesis, properties and applications. *Chem. Eng. J.* **185–186**, 1–22 (2012).
14. Pei, Z., Xu, H. & Zhang, Y. Preparation of Cr_2O_3 nanoparticles via C_2H_5OH hydrothermal reduction. *J. Alloys Compd.* **468**, 5–8 (2009).
15. Li, L., Zhu, Z., Yao, X., Lu, G. & Yan, Z. Synthesis and characterization of chromium oxide nanocrystals via solid thermal decomposition at low temperature. *Micropor. Mesopor. Mat.* **112**, 621–626 (2008).
16. Lima, M. D., Bonadimann, R., Andrade, M. J., Toniolo, J. C. & Bergmann, C. P. Evaluation of two different methods to synthesize cobalt-aluminate spinel. *J. Eur. Ceram. Soc.* **26**, 1213–1220 (2006).
17. Pinna, N., Garnweitner, G., Antonietti, M. & Niederberger, M. Non-aqueous synthesis of high-purity metal oxide nanopowders using an ether elimination process. *Adv. Mater.* **16**, 2196–2200 (2004).
18. Kim, D. W., Shin, S. I., Lee, J. D. & Oh, S. G. Preparation of chromia nanoparticles by precipitation–gelation reaction. *Mater. Lett.* **58**, 894–1898 (2004).
19. Tsuzuki, T. & Mc Cormick, P. G. Synthesis of Cr_2O_3 nanoparticles by mechanochemical processing. *Acta Mater.* **48**, 2795–2801 (2000).
20. Zhong, Z. C., Cheng, R. H., Bosley, J., Dowben, P. A. & Sellmyer, D. J. Fabrication of chromium oxide nanoparticles by laser-induced deposition from solution. *Appl. Surf. Sci.* **181**, 196–202 (2001).
21. Mougin, J., Le Bihan, T. & Lucazeau, G. High-pressure study of Cr_2O_3 obtained by high-temperature oxidation by X-ray diffraction and Raman spectroscopy. *J. Phys. Chem. Solids.* **62**, 553–563 (2001).
22. Sone, B., Manikandan, E., Gurib-Fakim, A. & Maaza, M. Single-phase α-Cr_2O_3 nanoparticles' green synthesis using *Callistemon viminalis*' red flower extract. *Green Chem. Lett. Rev.* **9**, 85–90 (2016).
23. Cuong, H. N. *et al.* New frontiers in the plant extract mediated biosynthesis of copper oxide (CuO) nanoparticles and their potential applications: A review. *Environ. Res.* **203**, 111858 (2022).
24. Marzban, A., Mirzaei, S. Z., Karkhane, M., Ghotekar, S. K. & Danesh, A. Biogenesis of copper nanoparticles assisted with seaweed polysaccharide with antibacterial and antibiofilm properties against methicillin-resistant *Staphylococcus aureus*. *J. Drug Deliv. Sci. Technol.* **74**, 103499 (2022).
25. Kashid, Y. *et al.* Bio-inspired sustainable synthesis of silver chloride nanoparticles and their prominent applications. *J. Indian Chem. Soc.* **99**, 100335 (2022).
26. Hassanisaadi, M. *et al.* Eco-friendly biosynthesis of silver nanoparticles using Aloysia citrodora leaf extract and evaluations of their bioactivities. *Mater. Today Commun.* **33**, 104183 (2022).
27. Garibo, D. *et al.* Green synthesis of silver nanoparticles using *Lysiloma acapulcensis* exhibit high-antimicrobial activity. *Sci. Rep.* **10**, 12805 (2020).
28. Sharma, U. R. & Sharma, N. Green synthesis, anti-cancer and corrosion inhibition activity of Cr_2O_3 nanoparticles. *Bioint. Res. App. Chem.* **11**, 8402–8412 (2021).
29. Mohamed, H. E. A. *et al.* Phyto-fabricated Cr_2O_3 nanoparticle for multifunctional biomedical applications. *Nanomedicine* **15**, 1653–1669 (2020).
30. Kotb, O. M., Abd El-Latif, F. M., Atawia, A. R., Saleh, S. S. & El-Gioushy, S. F. Green synthesis of chromium nanoparticles by aqueous extract of *Melia azedarach*, *Artemisia herba-alba* and bacteria fragments against *Erwinia amylovora*. *Asian J. Biotech. Biores. Tech.* **6**, 22–30 (2020).
31. Isacfranklin, M. *et al.* Single-phase Cr_2O_3 nanoparticles for biomedical applications. *Ceram. Int.* **46**, 19890–19895 (2020).
32. Tsegay, M. G., Gebretinsae, H. G. & Nuru, Z. Y. Structural and optical properties of green synthesized Cr_2O_3 nanoparticles. *Mater Today Proc.* **36**, 587–590 (2020).
33. Iqbal, J. *et al.* Facile green synthesis approach for the production of chromium oxide nanoparticles and their different in vitro biological activities. *Microsc. Res. Tech.* **83**, 706–719 (2020).
34. Sackey, J. *et al.* Biosynthesised black α-Cr_2O_3 nanoparticles; experimental analysis and density function theory calculations. *J. Alloys Compd.* **850**, 156671 (2021).
35. Ramesh, C., Kumar, K. T. M., Latha, N. & Ragunathan, V. Green synthesis of Cr_2O_3 nanoparticles using *Tridax procumbens* leaf extract and its antibacterial activity on *Escherichia coli*. *Curr. Nanosci.* **8**, 603–607 (2012).
36. Patra, J. K. & Baek, K.-H. Green nanobiotechnology: Factors affecting synthesis and characterization techniques. *J. Nanomater.* **2014**, 417305 (2014).
37. Pradeep, M., Kruszka, D., Kachlicki, P., Mondal, D. & Franklin, G. Uncovering the phytochemical basis and the mechanism of plant extract-mediated eco-friendly synthesis of silver nanoparticles using ultra-performance liquid chromatography coupled with a photodiode array and high-resolution mass spectrometry. *ACS Sustain. Chem. Eng.* **10**, 562–571 (2022).

38. Singh, P. P., Jaiswal, A. K., Kumar, A., Gupta, V. & Rakish, B. Untangling the multi-regime molecular mechanism of verbenol-chemotype Zingiber of cinale essential oil against *Aspergillus favus* and afatoxin B_1. *Sci. Rep.* **11**, 6832 (2021).
39. Gao, X. *et al.* Transformation of Chitin and Waste Shrimp shells into acetic acid and pyrrole. *ACS Sustain. Chem. Eng.* **4**, 3912–3920 (2016).
40. Chen, X., Chew, S. L., Kerton, F. M. & Yan, N. Direct conversion of chitin into a *N*-containing furan derivative. *Green Chem.* **16**, 2204–2212 (2014).
41. Singh, H. & Rajput, J. K. Co(II) anchored glutaraldehyde crosslinked magnetic chitosan nanoparticles (MCS) for synthesis of 2,4,5-trisubstituted and 1,2,4,5-tetrasubstituted imidazoles. *Appl. Organomet. Chem.* **32**, e3989 (2018).
42. Marzouk, A. A., Abu-Dief, A. M. & Abdelhamid, A. A. Hydrothermal preparation and characterization of $ZnFe_2O_4$ magnetic nanoparticles as an efficient heterogeneous catalyst for the synthesis of multi-substituted imidazoles and study of their anti-inflammatory activity. *Appl. Organomet. Chem.* **32**, e3794 (2018).
43. Takle, A. K. *et al.* The identification of potent and selective imidazole-based inhibitors of B-Raf kinase. *Bioorg. Med. Chem. Lett.* **16**, 378–381 (2006).
44. Balalaie, S., Arabanian, A. & Hashtroudi, M. S. Zeolite HY and Silica gel as new and efficient heterogenous catalysts for the synthesis of triarylimidazoles under microwave irradiation. *Monatsh. Fur. Chem.* **131**, 945–948 (2000).
45. Siddiqui, S. A. *et al.* Room temperature ionic liquid promoted improved and rapid synthesis of 2,4,5-triaryl imidazoles from aryl aldehydes and 1,2-diketones or α-hydroxyketone. *Tetrahedron* **61**, 3539–3546 (2005).
46. Shaabani, A., Rahmati, A., Aghaaliakbari, B. & Safaei-Ghomi, J. 1,1,3,3-*N*,*N*,*N*′,*N*′-Tetramethylguanidinium trifluoroacetate ionic liquid–promoted efficient one-pot synthesis of trisubstituted imidazoles. *Synth. Commun.* **36**, 65–70 (2006).
47. Kidwai, M., Mothsra, P., Bansal, V. & Goyal, R. Efficient elemental iodine catalyzed one-pot synthesis of 2,4,5-triarylimidazoles. *Monatsh. Fur. Chem.* **137**, 1189–1194 (2006).
48. Sangshetti, J. N., Kokare, N. D., Kothakar, S. A. & Shinde, D. B. Sodium Bisulfite as an efficient and inexpensive catalyst for the one-pot synthesis of 2,4,5-triaryl-1*H*-imidazoles from benzil or benzoin and aromatic aldehydes. *Monatsh. Fur. Chem.* **139**, 125–127 (2008).
49. Sharma, G. V. M., Jyothi, Y. & Lakshmi, P. S. efficient room-temperature synthesis of tri- and tetrasubstituted imidazoles catalyzed by $ZrCl_4$. *Synth. Commun.* **36**, 2991–3000 (2006).
50. Wang, L. M. *et al.* Ytterbium triflate as an efficient catalyst for one-pot synthesis of substituted imidazoles through three-component condensation of benzil, aldehydes and ammonium acetate. *J. Fluorine Chem.* **127**, 1570–1573 (2006).
51. Balalaie, S., Hashemi, M. M. & Akhbari, M. A. A novel one-pot synthesis of tetrasubstituted imidazoles under solvent-free conditions and microwave irradiation. *Tetrahedron Lett.* **44**, 1709–1711 (2003).
52. Shelke, K., Kakade, G., Shingate, B. & Shingare, M. Microwave induced one-pot synthesis of 2,4,5-tri aryl imidazoles using glyoxylic acid as a catalyst under solvent free condition. *Rasayan J. Chem.* **1**, 489–494 (2008).
53. Sharma, S. D., Hazarika, P. & Konwar, D. An efficient and one-pot synthesis of 2,4,5-trisubstituted and 1,2,4,5-tetrasubstituted imidazoles catalyzed by $InCl_3.3H_2O$. *Tetrahedron Lett.* **49**, 2216–2220 (2008).
54. Hangirgekar, S. P., Kumbhar, V. V., Shaikh, A. L. & Bhairuba, I. A. One-pot synthesis of 2,4,5-trisubstituted imidazoles using cupric chloride as a catalyst under solvent free conditions. *Der Pharma Chemica.* **6**, 164–168 (2014).
55. Kafi-Ahmadi, L., Poursattar Marjani, A. & Nozad, E. Ultrasonic-assisted preparation of Co_3O_4 and Eu-doped Co_3O_4 nanocatalysts and their application for solvent-free synthesis of 2-amino-4*H*-benzochromenes under microwave irradiation. *Appl. Organomet. Chem.* **35**, e6271 (2021).
56. Majidi Arlan, F., Poursattar Marjani, A., Javahershenas, R. & Khalafy, J. Recent developments in the synthesis of polysubstituted pyridines via multicomponent reactions using nanocatalysts. *New. J. Chem.* **45**, 12328–12345 (2021).
57. Azimi, F., Poursattar Marjani, A. & Keshipour, S. Fe(II)-phthalocyanine supported on chitosan aerogel as a catalyst for oxidation of alcohols and alkyl arenes. *Sci. Rep.* **11**, 23769 (2021).
58. Khashaei, M., Kafi-Ahmadi, L., Khademinia, S., Poursattar Marjani, A. & Nozad, E. A facile hydrothermal synthesis of high-efficient NiO nanocatalyst for preparation of 3,4-dihydropyrimidin-2(1*H*)-ones. *Sci. Rep.* **12**, 8585 (2022).
59. Parsa Habashi, B. & Poursattar Marjani, A. *N*-methylpyrrolidine as an effective organocatalyst for the regioselective synthesis of 3-hydroxy-3,5/6-di-aryl-1*H*-imidazo[1,2-*a*]imidazol-2(3*H*)-ones. *Res. Chem. Intermed.* **48**, 2325–2336 (2022).
60. Kafi-Ahmadi, L., Khademinia, S., Poursattar Marjani, A. & Gozali Balkanloo, P. Fabrication of 5-aryl-1*H*-tetrazoles derivatives by solid-state synthesized $MgFe_2O_4$ and $MgFe_2Zn_xO_{4+\delta}$ heterogeneous nanocatalysts. *Res. Chem. Intermed.* **48**, 2973–2986 (2022).
61. Chen, L. *et al.* Three-dimensional morphology control during wet chemical synthesis of porous chromium oxide spheres. *ACS Appl. Mater. Interfaces.* **1**, 1931–1937 (2009).
62. Farzaneh, F. & Najafi, M. Synthesis and characterization of Cr_2O_3 nanoparticles with triethanolamine in water under microwave irradiation. *J. Sci. Islam. Repub. Iran.* **22**, 329–333 (2011).
63. Chavan, H. V. & Narale, D. K. Synthesis of 2,4,5-triaryl and 1,2,4,5-tetraaryl imidazoles using silica chloride as an efficient and recyclable catalyst under solvent-free conditions. *C. R. Chim.* **17**, 980–984 (2013).
64. Chavan, L. D. & Shankarwar, S. G. KSF supported 10-molybdo-2-vanadophosphoric acid as an efficient and reusable catalyst for one-pot synthesis of 2,4,5-trisubstituted imidazole derivatives under solvent-free condition. *Chin. J. Catal.* **36**, 1054–1059 (2015).
65. Khazaei, H. A., Alavi Nik, A., Ranjbaran, A. R. & Moosavi-Zare,. Synthesis, characterization and application of $Ni_{0.5}Zn_{0.5}Fe_2O_4$ nanoparticles for the one pot synthesis of triaryl-1*H*-imidazoles. *RSC Adv.* **6**, 78881–78886 (2016).
66. Nagalakshmi, G. Synthesis and pharmacological evaluation of 2-(4-halosubstituted phenyl)-4,5-diphenyl-1*H*-imidazoles. *Eur. J. Chem.* **5**, 447–452 (2008).
67. Gorsd, M., Sathicq, G., Romanelli, G., Pizzio, L. & Blanco, M. Tungstophosphoric acid supported on core-shell polystyrene-silica microspheres or hollow silica spheres catalyzed trisubstituted imidazole synthesis by multicomponent reaction. *J. Mol. Catal. A. Chem.* **420**, 294–302 (2016).
68. Chundawat, T. S., Sharma, N., Kumari, P. & Bhagat, S. Microwave-assisted nickel-catalyzed one-pot synthesis of polysubstituted imidazoles. *Synlett* **27**, 404–408 (2016).
69. Thimmaraju, N. & Shamshuddin, S. Z. M. Synthesis of 2,4,5-trisubstituted imidazoles, quinoxalines and 1,5-benzodiazepines over eco-friendly and highly efficient ZrO_2-Al_2O_3 catalyst. *RSC Adv.* **6**, 60231–60243 (2016).
70. Shitole, B. V., Shitole, N. V., Ade, S. B. & Kakde, G. K. Microwave-induced one-pot synthesis of polysubstituted imidazoles using Rochelle salt as a green novel catalyst. *Orbital. E- J. Chem.* **7**, 240–244 (2015).
71. Mardani, H. R., Forouzani, M. & Emami, R. Efficient and green synthesis of trisubstituted imidazoles by magnetically nanocatalyst and microwave assisted. *Asian J. Green Chem.* **3**, 525–535 (2019).
72. Safari, J., Dehghan Khalili, S. & Banitab, S. H. Three-component, one-pot synthesis of polysubstituted imidazoles catalyzed by $TiCl_4$–SiO_2 under conventional heating conditions or microwave irradiation. *Synth. Commun.* **41**, 2359–2373 (2011).
73. Asressu, K. H., Chan, C.-K. & Wang, C.-C. TMSOTf-catalyzed synthesis of trisubstitutedimidazoles using hexamethyldisilazane as a nitrogen source under neat and microwave irradiation conditions. *RSC Adv.* **11**, 28061–28071 (2021).
74. Alikarami, M. & Amozad, M. One-pot synthesis of polysubstituted imidazole derivatives catalyzed by btppc under solvent-free conditions. *Bull. Chem. Soc. Ethiop.* **31**, 177–184 (2017).
75. Safari, J., Gandomi-Ravandi, S. & Akbari, Z. Improving methodology for the preparation of highly substituted imidazoles using nano-$MgAl_2O_4$ as catalyst under microwave irradiation. *Iran. J. Catal.* **3**, 33–39 (2013).

Acknowledgements
The authors would like to acknowledge the support received from the Research Council of Urmia University.

Author contributions
L.K.-A.: conceptualization, data curation, formal analysis, funding acquisition, investigation, methodology, project administration, resources, supervision, validation, visualization, writing-original draft, and writing-review and editing. S.K.: conceptualization, data curation, formal analysis, investigation, methodology, supervision, and writing-review and editing. A.P.M.: conceptualization, data curation, formal analysis, investigation, methodology, supervision, validation, visualization, and writing-review and editing. E.N.: Investigation, writing–review and editing.

Competing interests
The authors declare no competing interests.

Additional information
Supplementary Information The online version contains supplementary material available at https://doi.org/10.1038/s41598-022-24364-6.

Correspondence and requests for materials should be addressed to A.P.M.